



# Rag–Ragulator is the central organizer of the physical architecture of the mTORC1 nutrient-sensing pathway

Max L. Valenstein<sup>a,b,c,d,1,2</sup>, Pranav V. Lalgudi<sup>b,c,1</sup>, Xin Gu<sup>b,c,d,1</sup>, Jibril F. Kedir<sup>b,c,d</sup>, Martin S. Taylor<sup>d,e,f,g,h</sup>, Raghu R. Chivukula<sup>a,d,i,j,k</sup>, and David M. Sabatini<sup>l,2</sup> 

Affiliations are included on p. 12.

Contributed by David M. Sabatini; received December 24, 2023; accepted July 12, 2024; reviewed by Brendan Manning and Reuben Shaw

The mechanistic target of rapamycin complex 1 (mTORC1) pathway regulates cell growth and metabolism in response to many environmental cues, including nutrients. Amino acids signal to mTORC1 by modulating the guanine nucleotide loading states of the heterodimeric Rag GTPases, which bind and recruit mTORC1 to the lysosomal surface, its site of activation. The Rag GTPases are tethered to the lysosome by the Ragulator complex and regulated by the GATOR1, GATOR2, and KICSTOR multiprotein complexes that localize to the lysosomal surface through an unknown mechanism(s). Here, we show that mTORC1 is completely insensitive to amino acids in cells lacking the Rag GTPases or the Ragulator component p18. Moreover, not only are the Rag GTPases and Ragulator required for amino acids to regulate mTORC1, they are also essential for the lysosomal recruitment of the GATOR1, GATOR2, and KICSTOR complexes, which stably associate and traffic to the lysosome as the “GATOR” supercomplex. The nucleotide state of RagA/B controls the lysosomal association of GATOR, in a fashion competitively antagonized by the N terminus of the amino acid transporter SLC38A9. Targeting of Ragulator to the surface of mitochondria is sufficient to relocalize the Rags and GATOR to this organelle, but not to enable the nutrient-regulated recruitment of mTORC1 to mitochondria. Thus, our results reveal that the Rag–Ragulator complex is the central organizer of the physical architecture of the mTORC1 nutrient-sensing pathway and underscore that mTORC1 activation requires signal transduction on the lysosomal surface.

mTOR signaling | nutrient sensing | biochemistry

The mTORC1 pathway is a master regulator of cell growth and metabolism that integrates varied environmental signals, is dysregulated in diseases including cancer and diabetes, and plays a key role in the aging process. Nutrients and insulin signal to mTORC1 through multiple distinct lysosomally localized GTPases, the Rags and Rheb (1–5), respectively. The nucleotide state of the heterodimeric Rag GTPases (consisting of RagA or RagB bound to RagC or RagD), which are anchored on the lysosomal surface by the pentameric Ragulator complex, transmits nutrient availability to mTORC1. Upon nutrient stimulation, the RagA/B<sup>GTP</sup>-RagC/D<sup>GDP</sup> configuration recruits mTORC1 to the lysosomal surface via a direct interaction with its Raptor subunit (6–9). In contrast, nutrient deprivation promotes the RagA/B<sup>GDP</sup>-RagC/D<sup>GTP</sup> configuration, which excludes mTORC1 from the lysosomal surface. At the lysosome, GTP-loaded Rheb directly binds to mTORC1 and stimulates its kinase activity in response to growth factors like insulin, ensuring that mTORC1 is active only when both nutrients and growth factors are present (10).

A network of lysosomal multiprotein complexes, including GATOR1, KICSTOR, and GATOR2, regulates the nucleotide configuration of the Rag GTPases. The trimeric GATOR1 complex (DEPDC5, Nprl2, Nprl3) interacts with KICSTOR (SZT2, c12orf66, ITFG2, KPTN) and functions as a GTPase activating protein (GAP) toward RagA/B, and thus inhibits mTORC1 during nutrient starvation (11–16). GATOR1 and KICSTOR interact with GATOR2 (Mios, WDR24, WDR59, Seh1L, Sec13), which promotes mTORC1 activation by opposing GATOR1 through an unknown molecular mechanism (11, 17). GATOR2 receives inhibitory signals from the cytosolic nutrient sensors Sestrin1/2 and CASTOR1, which directly bind leucine and arginine, respectively (18–21). An additional nutrient sensor, SAMTOR, inhibits mTORC1 activation in the absence of S-adenosylmethionine by associating with GATOR1 and KICSTOR and the recently identified cholesterol sensor, LYCHOS, stimulates mTORC1 through GATOR1 (22, 23). Accordingly, diverse nutrients signal through the GATOR1, KICSTOR, and GATOR2 complexes to set the nucleotide configuration of the Rag GTPases. The Rag GTPases also bind to the FLCN–FNIP2 complex, which functions as a GAP toward RagC/D and

## Significance

The mTORC1 signaling pathway coordinates cellular metabolism with nutrient availability to regulate cell growth. Nutrients, such as amino acids, signal to mTORC1 through the Rag GTPases, which reside on the surface of the lysosome. Several large multiprotein complexes, including GATOR1, KICSTOR, and GATOR2, control the Rag GTPases, but it remains unknown how these complexes access the lysosomal surface. We show that the Rag GTPases and the associated Ragulator complex anchor their own regulators onto the lysosome. Our findings highlight the Rag–Ragulator complex as the central actor in both the information transduction and physical architecture of this critical nutrient-sensing signaling pathway.

Reviewers: B.D.M., Harvard School of Public Health; and R.J.S., Salk Institute for Biological Studies.

The authors declare no competing interest.

Copyright © 2024 the Author(s). Published by PNAS. This article is distributed under [Creative Commons Attribution-NonCommercial-NoDerivatives License 4.0 \(CC BY-NC-ND\)](https://creativecommons.org/licenses/by-nc-nd/4.0/).

<sup>1</sup>M.L.V., P.V.L., and X.G. contributed equally to this work.

<sup>2</sup>To whom correspondence may be addressed. Email: mlvalenstein@mgb.org or david.sabatini@iocb.cz.

This article contains supporting information online at <https://www.pnas.org/lookup/suppl/doi:10.1073/pnas.2322755121/-/DCSupplemental>.

Published August 20, 2024.

principally promotes phosphorylation, in part by mTORC1, of the TFEB/TFE3 (24–27) transcription factors.

Given the central role of GATOR1, KICSTOR, and GATOR2 in nutrient sensing by mTORC1, it is important to understand how these large, multiprotein complexes access and engage one another on the lysosomal surface. While the KICSTOR complex is critical for the lysosomal localization of GATOR1 (15, 16), it remains unclear how KICSTOR and GATOR2 are recruited to the lysosome or whether the lysosomal surface enables interactions between these complexes. Here, we adapt the Lyso-IP and MITO-IP methods for the rapid isolation of lysosomes and mitochondria, respectively, to study how these complexes localize to the lysosome (28, 29).

We find that Ragulator and the Rag GTPases are not only required for mTORC1 to sense amino acids, but also for recruitment of the GATOR supercomplex, comprising GATOR1, KICSTOR, and GATOR2, to the lysosome. These results place

Ragulator and the Rag GTPases at the center of both the structural organization and information transduction of the nutrient-sensing pathway upstream of mTORC1.

## Results

We used CRISPR-mediated genome editing to generate HEK293T cell lines lacking core components of each complex in the nutrient-sensing pathway (p18, Ragulator; RagA and RagB or RagC and RagD, Rag GTPases; Mios, GATOR2; DEPDC5 or Nprl2, GATOR1; SZT2, KICSTOR, Fig. 1A). In our experience, it can be challenging to isolate clones completely lacking positive regulators of mTORC1 signaling, including Ragulator, the Rag GTPases, and GATOR2, because they have reduced fitness and grow more slowly than those with only partial knockdowns. To avoid selecting clones with incomplete disruption of the expression of positive regulators, we undertook several measures, including

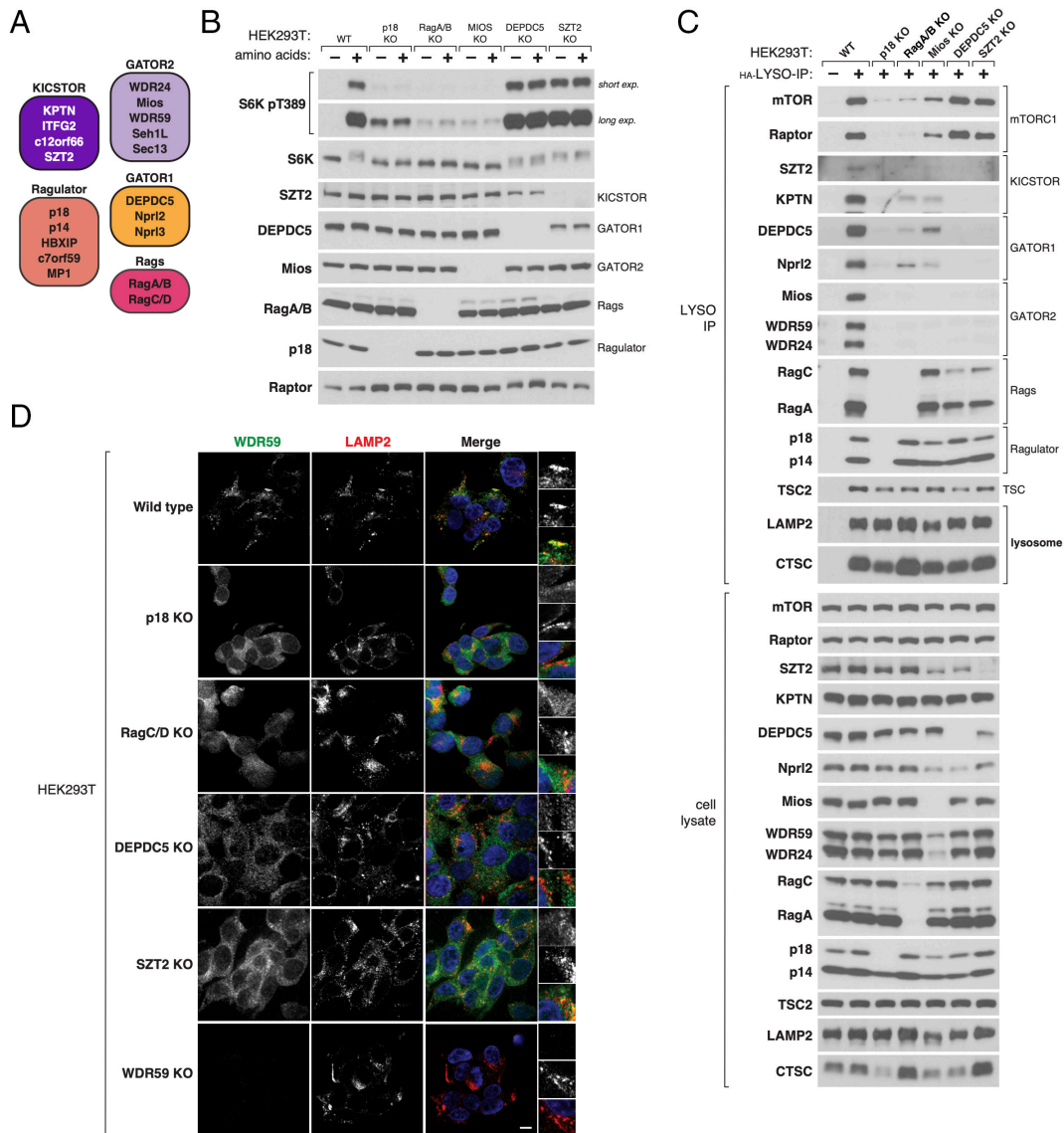


**Fig. 1.** Rag and Ragulator are required to recruit GATOR to lysosomes. (A) Schematics depicting the components of the core mTORC1 nutrient-sensing pathway complexes. (B) Loss of core nutrient-sensing pathway components renders mTORC1 signaling insensitive to amino acid deprivation or stimulation. HEK293T cell clones of the indicated genotypes were starved for amino acids for 60 min and restimulated or not with amino acids for 15 min prior to harvest. Cell lysates were analyzed by immunoblotting for the levels and phosphorylation states of the indicated proteins. (C) The Ragulator and Rag GTPases are required for the presence of GATOR1, KICSTOR, and GATOR2 on immunopurified lysosomes. Lysosomes were immunopurified from HEK293T cells of the indicated genotypes expressing TMEM192-3xHA (HA-LYSO-IP) and analyzed by immunoblotting for the levels of the indicated proteins. (D) The Ragulator and Rag GTPases are required for the colocalization of GATOR2 with lysosomes. HEK293T cells of the indicated genotypes were fixed and LAMP2 and the GATOR2 component WDR59 were detected by immunofluorescence (The scale bar denotes 10 μm.)

first screening candidate knockout clones by genomic sequencing and then validating them by long-exposure immunoblotting (*Materials and Methods*). As expected, disruption of the Ragulator, Rag GTPases, or GATOR2 rendered mTORC1 unable to sense the presence of amino acids, whereas mTORC1 remained active in the absence of amino acids in cells lacking intact GATOR1 or KICSTOR (Fig. 1*B* and *SI Appendix, Fig. S1A*). Cells lacking either Ragulator, the Rag GTPases, or GATOR2 exhibited a higher baseline level of mTORC1 signaling, possibly due to increased expression of the mTORC1 component Raptor (Fig. 1*B* and *SI Appendix, Fig. S1A*) or compensatory changes in Akt-TSC-Rheb signaling, which has been shown to promote nutrient-independent mTORC1 activity in the absence of the Rags (30).

We immunopurified lysosomes from each knockout cell line using a Lyso-IP protocol optimized to capture proteins weakly associated with the lysosomal membrane (Fig. 1*C* and *SI Appendix, Fig. S1B*). The immunoisolation of lysosomes from nutrient-stimulated wild-type HEK293T cells recovered all five nutrient-sensing complexes as well as mTORC1. In line with prior reports, disruption of either Ragulator or the Rag GTPases abolished the lysosomal recruitment of mTORC1 and the amount of mTORC1 captured on lysosomes correlated with mTORC1 activity in each knockout cell line (Fig. 1*B* and *C* and *SI Appendix, Fig. S1B*) (9).

To our surprise, we found that Ragulator and the Rag GTPases were also required for GATOR1, KICSTOR, and GATOR2 to copurify with the isolated lysosomes (Fig. 1*C* and *SI Appendix, Fig. S1B*). Furthermore, we determined that GATOR1, KICSTOR, and GATOR2 were codependent on each other to stably associate with lysosomes. Disruption of either GATOR1 or KICSTOR abolished the lysosomal recruitment of GATOR2. Consistent with the inhibitory effect of GATOR2 depletion on mTORC1 signaling, a small amount of GATOR1 and KICSTOR remained associated with the lysosome even in the cells lacking the GATOR2 component Mios (Fig. 1*C* and *SI Appendix, Fig. S1B*). None of the nutrient-sensing complexes were required for the Tuberous Sclerosis Complex (TSC) complex that regulates the Rheb GTPases to interact with the lysosome (Fig. 1*C*), although the loss of Ragulator, Rag GTPases, and GATOR1 did slightly decrease the amount of TSC2 recovered with lysosomes.

In agreement with our observations using lysosomal immunocapture, loss of intact Ragulator, Rag GTPases, GATOR1, or KICSTOR disrupted the subcellular distribution of the GATOR2 component WDR59 as assessed by immunofluorescence microscopy of fixed cells (Fig. 1*D*). Thus, the decreased lysosomal capture of GATOR2 reflects its impaired lysosomal recruitment rather than a diminished stability and subsequent dissociation from lysosomes during the process of organellar immunopurification. Taken together, these results indicate that the Ragulator and Rag GTPases are not only required for the lysosomal recruitment of mTORC1, but also of GATOR1, KICSTOR, and GATOR2, which in turn are mutually dependent on each other to associate with the lysosome.

Given these interdependent relationships, we wondered whether a lysosomal localization is necessary to scaffold the interactions between GATOR1, KICSTOR, and GATOR2. To evaluate this, we assessed the capacity of each complex to coimmunoprecipitate the others from our cell lines lacking core pathway components. We found that loss of either the Ragulator component p18 or of both RagA and RagB did not affect the interactions between GATOR1, KICSTOR, and GATOR2 (Fig. 2*A–C*). These results suggest that GATOR1, KICSTOR, and GATOR2 stably assemble independently of their recruitment to the lysosomal surface. Consistent with previous reports, GATOR1 and KICSTOR remained associated upon loss of GATOR2, but neither GATOR1

nor KICSTOR were required for the integrity of the GATOR2 complex (Fig. 2*A–C*) (15, 16). Accordingly, we propose that GATOR1, KICSTOR, and GATOR2 form a functional supercomplex, which we designate “GATOR,” comprising two independently stable subcomplexes: GATOR1-KICSTOR and GATOR2.

To determine the relative stoichiometries of GATOR, Rag, and Ragulator complexes, we generated HEK293T cell lines with a 3xFLAG epitope knocked into the coding sequence of a central component of each complex (*SI Appendix, Fig. S2*). In agreement with public protein abundance datasets (31), we found that the expression of core components of GATOR1, GATOR2, and KICSTOR is substoichiometric relative to that of the Rags and Ragulator. The molar excess of Rags and Ragulator may be necessary to anchor numerous multiprotein assemblies, including mTORC1 and GATOR, to the lysosome in a noncompetitive manner.

We also assessed whether the interactions between the GATOR subcomplexes and the cytosolic nutrient sensors Sestrin1/2, CASTOR1, and SAMTOR require access to the lysosomal surface. We observed no difference in the nutrient-regulated interactions between GATOR2 and Sestrin1/2 and CASTOR1 (Fig. 2*D*) or between GATOR1-KICSTOR and SAMTOR (Fig. 2*E*) in cells with or without the Ragulator component p18. Thus, localization to the lysosome is not required for regulated interaction between GATOR and established cytosolic nutrient sensors. Together, our results suggest that a functional GATOR supercomplex traffics to and from the lysosome rather than assembles on it (Fig. 2*F*).

As the Rag GTPases are necessary for the lysosomal recruitment of GATOR, we hypothesized that the nucleotide state of the Rags should influence GATOR's lysosomal localization. Indeed, when we immunopurified lysosomes from amino acid-starved or -stimulated cells we found that amino acids subtly diminished the amount of cocaptured GATOR components Mios, DEPDC5, and KPTN (Fig. 3*A*). More dramatically, we found greater lysosomal capture of GATOR in RagA/B-deficient cells reconstituted with an obligatorily GDP-bound RagB variant than in those expressing a GTP-bound variant (Fig. 3*B*). Moreover, massive overexpression of a constitutively GTP-bound mutant of RagB reduced the capture of lysosomal GATOR in wild-type HEK293T cells (*SI Appendix, Fig. S3A*) as did complementation of Nprl2-deficient cells with a catalytically dead mutant of Nprl2 (R78A) that eliminates the GAP activity of GATOR1 (Fig. 3*C* and *SI Appendix, Fig. S3B*). These results indicate that GDP-loading of RagA/B promotes the interaction of GATOR with the lysosome.

GTP-loading of RagA/B has been reported to destabilize the interaction between the Rags and Ragulator (Fig. 3*B*), which may contribute to these observations (32, 33). To evaluate this possibility, we transiently expressed and isolated nucleotide-binding mutant forms of the Rag GTPases and found that the GDP-loaded variant of RagB most effectively coimmunoprecipitated GATOR (Fig. 3*D*). Thus, GDP-loaded RagA/B increases the amount of GATOR on the lysosome by promoting both Rag–GATOR and Rag–Ragulator interactions.

Multiple factors interact directly with the Rag GTPases including the lysosomal transporter SLC38A9, which binds the Rags via its N-terminal domain (34–36). Like GATOR, SLC38A9 preferentially interacts with the GDP-loaded form of RagA/B (34–36). SLC38A9 was initially described as a positive regulator of mTORC1, as mTORC1 signaling in cells overexpressing its N-terminal domain was found to be resistant to amino acid deprivation (34–36). Paradoxically, however, the SLC38A9 N terminus stabilizes the GDP-bound configuration of RagA/B, which promotes a Rag state

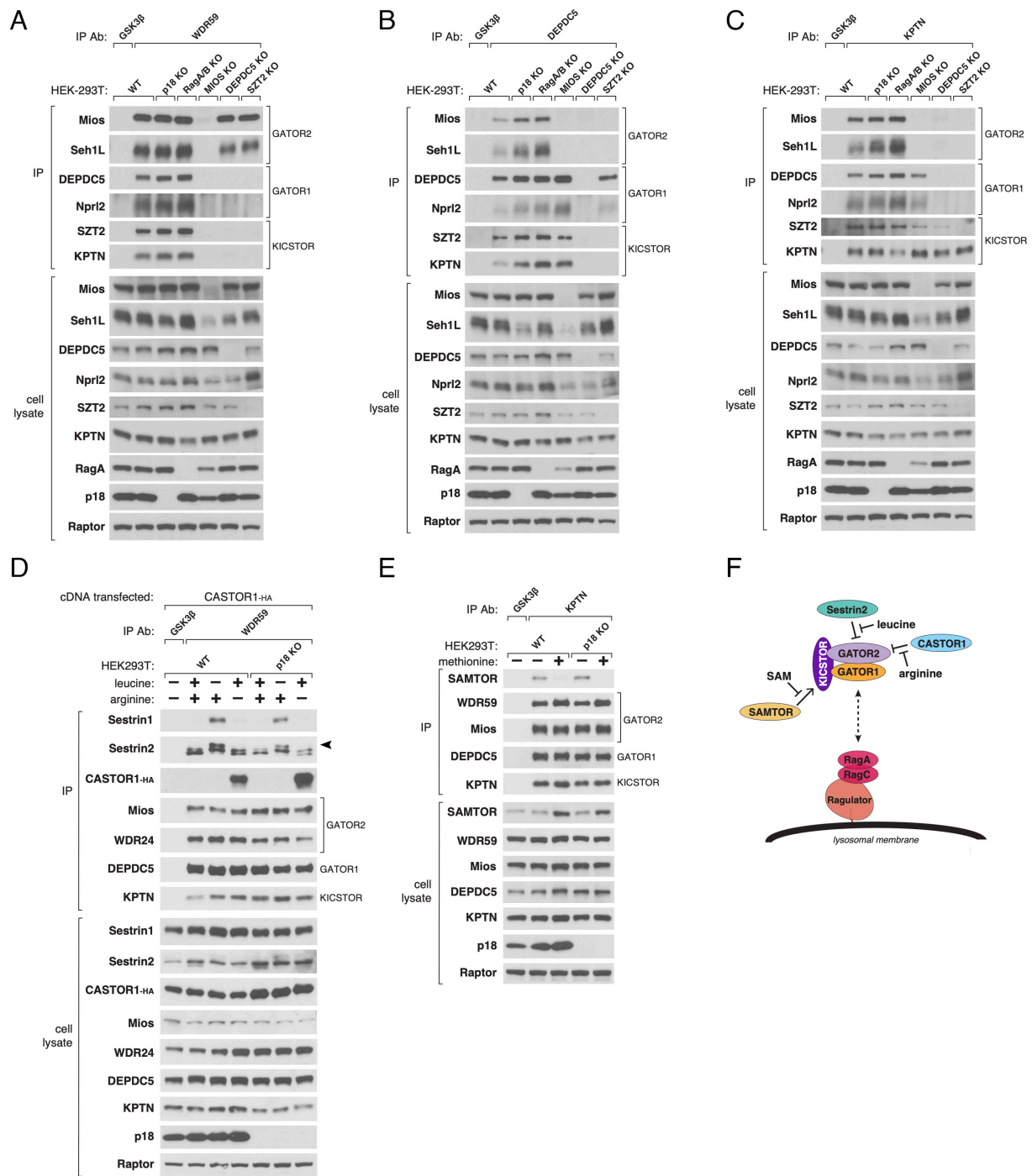


**Fig. 2.** The GATOR subcomplexes, and nutrient sensors, can interact with each other in the absence of their lysosomal localization. (A)–(C) The Ragulator and Rag GTPases are not required for GATOR1, KICSTOR, and GATOR2 to interact. Immunoprecipitates were prepared from HEK293T cells of the indicated genotypes with antibodies against (A) WDR59, (B) DEPDC5, or (C) KPTN and analyzed by immunoblotting for the levels of the indicated proteins. (D) Ragulator is not required for GATOR2 to interact with Sestrin1, Sestrin2, or CASTOR1 in a nutrient-regulated manner. HEK293T cells of the indicated genotypes were starved for either leucine or arginine for 60 min and restimulated or not with leucine or arginine, respectively, for 15 min prior to harvest. Anti-WDR59 immunoprecipitates were prepared from cells that transiently expressed the indicated protein and were analyzed by immunoblotting for the indicated proteins. (E) Ragulator is not required for KICSTOR to interact with SAMTOR in a nutrient-regulated manner. HEK293T cells of the indicated genotypes were starved for methionine or transitioned to fresh media containing methionine for 120 min prior to harvest. Anti-KPTN immunoprecipitates were prepared from cells and analyzed by immunoblotting for the indicated proteins. (F) Cartoon representation of the interactions between GATOR, nutrient sensors, and Rag-Gulagulator.

that antagonizes mTORC1 activation (37). We wondered whether overexpression of SLC38A9 could affect mTORC1 signaling by competing with GATOR for access to the Rag GTPases. Indeed, we found that coexpression of the SLC38A9 N-terminal domain disrupted the interaction between the Rag GTPases and GATOR in a dose-dependent manner (Fig. 4A). We generated a cell line stably expressing the N-terminal domain of SLC38A9 and

confirmed that it renders mTORC1 signaling partially resistant to amino acid starvation (Fig. 4B). Lysosomes immunopurified from these cells contained significantly less GATOR than from those expressing a control protein (Fig. 4C). Thus, massive overexpression of SLC38A9 promotes resistance to amino acid deprivation by displacing GATOR, including its catalytic GATOR1 subcomplex, from the lysosome (Fig. 4D). These results clarify how the SLC38A9

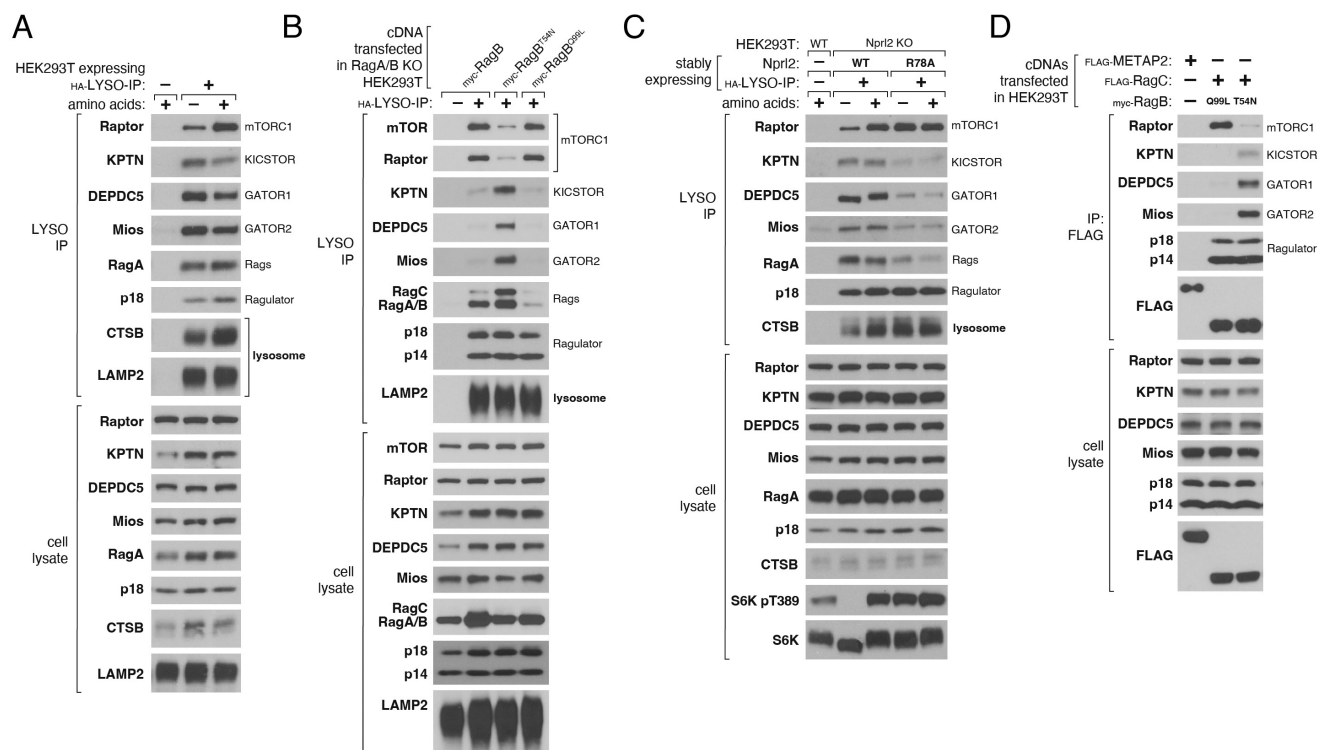


**Fig. 3.** The Rag nucleotide state influences the lysosomal abundance of GATOR. (A) Amino acids partially decrease the lysosomal abundance of GATOR. HEK293T cells were starved for amino acids for 60 min and restimulated or not with amino acids for 15 min prior to harvest. Lysosomes were immunopurified from cells expressing TMEM192-3xHA (HA-LYSO-IP) and analyzed by immunoblotting for the levels of the indicated proteins. (B) Expression of RagB nucleotide binding mutants alters the lysosomal abundance of GATOR. Lysosomes were immunopurified from HEK293T cells expressing TMEM192-3xHA (HA-LYSO-IP) and the indicated cDNAs and analyzed by immunoblotting for the levels of the indicated proteins. (C) Loss of GATOR1 catalytic activity decreases the lysosomal abundance of GATOR. HEK293T cells of the indicated genotypes were starved for amino acids for 60 min and restimulated or not with amino acids for 15 min prior to harvest. Lysosomes were immunopurified from cells expressing TMEM192-3xHA (HA-LYSO-IP) and analyzed by immunoblotting for the levels of the indicated proteins. (D) GATOR preferentially interacts with GDP-loaded RagB. Anti-FLAG immunoprecipitates were prepared from HEK293T cells transiently expressing the indicated proteins and analyzed by immunoblotting for the indicated proteins.

N-terminal domain can both function as a guanine nucleotide dissociation inhibitor (GDI) toward RagA/B *in vitro* and artificially activate mTORC1 signaling when overexpressed in cells. Consistent with these conclusions, we re-generated SLC38A9-deficient cells using CRISPR (Fig. 4E) and found no defect in nutrient-regulated mTORC1 signaling (Fig. 4F and G).

Given that the Ragulator and Rag GTPases are necessary to localize GATOR to the lysosome, we wondered whether they are sufficient to target it to a different subcellular compartment. To test this, we generated cells expressing either wild-type Ragulator component p18 (p18-WT) or a variant fused to the N-terminal domain of AKAP1, which targets it to the outer membrane of mitochondria (p18-M) (Fig. 5A). We verified that these constructs were present in the appropriate subcellular compartments by analyzing their colocalization with the lysosomal membrane marker LAMP2 and the outer mitochondrial membrane marker TOM20 (Fig. 5B and C). Using the Lyso-IP and MITO-IP methods, we isolated organelles from these cells and examined the abundances of the nutrient-sensing complexes (28, 29). Expression in p18-deficient cells of wild-type p18, but not mitochondria-targeted p18, restored the lysosomal capture of the Ragulator, Rag GTPases, and GATOR (Fig. 5D). In contrast, SLC38A9 and the v-ATPase component ATP6V0d1, which are integral lysosomal membrane proteins, did not require p18 to access the lysosome. Mitochondria isolated from cells expressing mito-targeted p18, but not wild-type p18, corecovered the Ragulator, Rag GTPases, and GATOR complexes (Fig. 5E). Thus, the Ragulator complex is sufficient to establish the subcellular localization of the Rags and GATOR.

We tested whether complementation of p18-deficient cells with mito-targeted p18 restored the regulation of mTORC1 signaling

by nutrients. Unlike complementation with wild-type p18, expression in the p18 knockout cells of mito-targeted p18 failed to restore amino acid-stimulated phosphorylation of either S6K1 or TFEB, the latter of which is phosphorylated by mTORC1 independently of the lysosomal Rheb GTPase (Fig. 6A) (25). As mTORC1 is capable of catalyzing substrate phosphorylation when it is artificially targeted to the mitochondria (25, 33), we speculated that these results may reflect the failure of mito-targeted Ragulator and Rags to recruit mTORC1 to the mitochondrial surface. Indeed, amino acids stimulated the lysosomal localization of mTORC1 in cells expressing wild-type p18 (Fig. 6B), but failed to promote significant mitochondrial localization of mTORC1 in cells expressing mito-targeted p18 (Fig. 6C). Similarly, amino acids did not potentiate the interaction between mito-targeted p18 and the mTORC1 component Raptor above the level observed in nutrient-starved cells (Fig. 6D).

Amino acid stimulation may fail to promote association of mTORC1 with mitochondria either because the mitochondrially localized Rag GTPases cannot acquire the nucleotide state necessary to recruit mTORC1 or because mTORC1 is unable to translocate to and dock on the mitochondrial surface. To evaluate these possibilities, we monitored the interaction between Ragulator and FLCN-FNIP2, which is disrupted by nutrient-dependent Rag nucleotide switching (24). We found that amino acid stimulation disrupted the interaction between Ragulator and FLCN-FNIP2 to a lesser degree in cells expressing mito-targeted p18 compared to those expressing wild-type p18 (Fig. 6D). This suggests that the Rag GTPase nucleotide configuration responds less dynamically to nutrients in cells expressing mito-targeted p18 than in those expressing wild-type p18. Consistently, overexpression of a

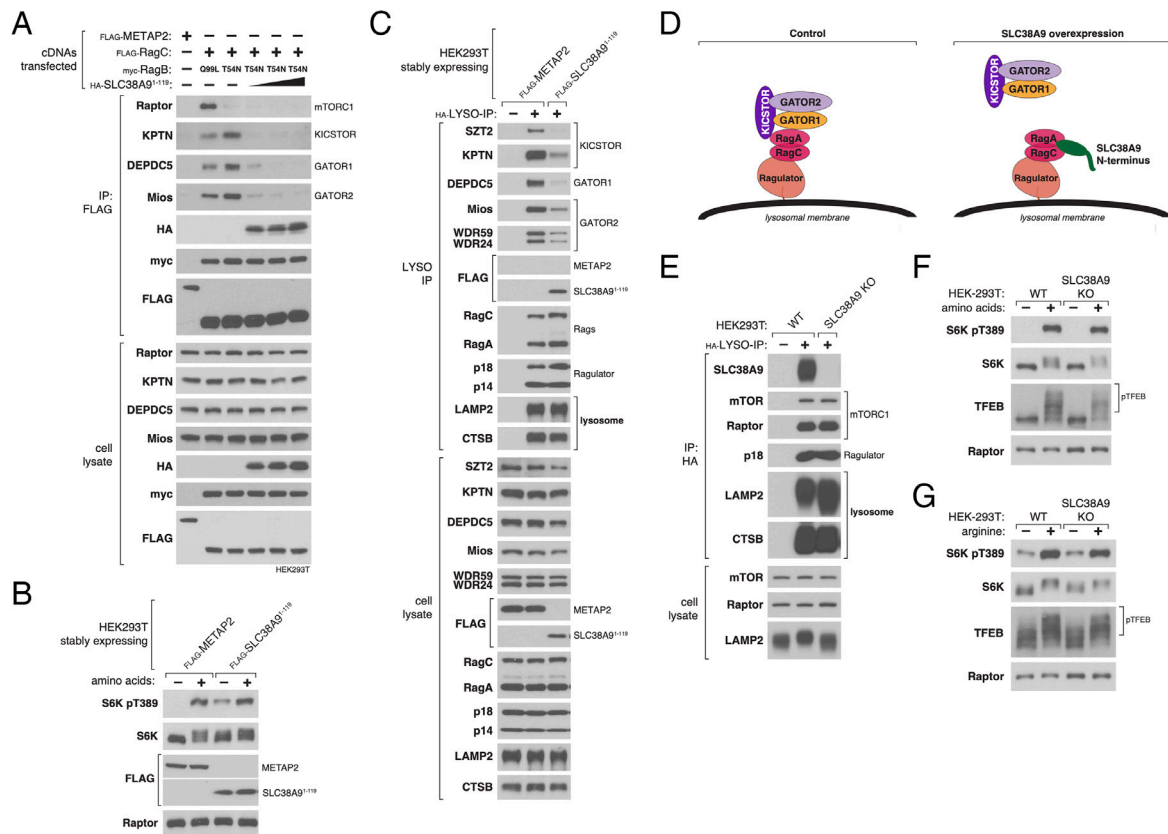


**Fig. 4.** Overexpression of the SLC38A9 N-terminal domain displaces GATOR from the lysosome. (A) The SLC38A9 N-terminal domain competes with GATOR for binding to the Rag GTPases. Anti-FLAG immunoprecipitates were prepared from HEK293T cells transiently expressing the indicated proteins and analyzed by immunoblotting for the indicated proteins. (B) Overexpression of the SLC38A9 N-terminal domain renders mTORC1 signaling resistant to amino acid deprivation. HEK293T cells of the indicated genotype were starved for amino acids for 60 min and restimulated or not with amino acids for 15 min prior to harvest. Cell lysates were analyzed by immunoblotting for the levels and phosphorylation states of the indicated proteins. (C) Overexpression of the SLC38A9 N-terminal domain displaces GATOR from the lysosome. Lysosomes were immunopurified from HEK293T cells of the indicated genotypes expressing TMEM192-3xHA (HA-LYSO-IP) and analyzed by immunoblotting for the levels of the indicated proteins. (D) Cartoon representation of the competition between the SLC38A9 N-terminal domain and GATOR for binding to the Rag GTPases. (E) CRISPR-Cas9-mediated stable loss of SLC38A9 does not affect recruitment of mTORC1 to the lysosome. Lysosomes were immunopurified from HEK293T cells of the indicated genotypes expressing TMEM192-3xHA (HA-LYSO-IP) and analyzed by immunoblotting for the levels of the indicated proteins. (F) Stable loss of SLC38A9 does not affect regulation of mTORC1 signaling by amino acids. HEK293T cell clones of the indicated genotypes were starved for amino acids for 60 min and restimulated or not with amino acids for 15 min prior to harvest. Cell lysates were analyzed by immunoblotting for the levels and phosphorylation states of the indicated proteins. (G) Stable loss of SLC38A9 does not affect regulation of mTORC1 signaling by arginine. HEK293T cell clones of the indicated genotype were starved for arginine for 60 min and restimulated or not with arginine for 15 min prior to harvest. Cell lysates were analyzed by immunoblotting for the levels and phosphorylation states of the indicated proteins.

GTP-loaded RagB variant enhanced association of mTORC1 with the lysosome or mitochondria in cells expressing wild-type or mito-targeted p18, respectively (Fig. 6 E and F). Disruption of GATOR1 component DEPDC5 also modestly increased the abundance of mTORC1 on mitochondria from cells expressing mito-targeted p18 (SI Appendix, Fig. S4A) but failed to promote recruitment of TFEB to that compartment or to stimulate nutrient-dependent TFEB phosphorylation (SI Appendix, Fig. S4 A and B). Together, these results suggest that mTORC1 does not accumulate on the mitochondria of cells expressing mito-targeted p18 primarily due to inadequate switching of the Rag GTPase nucleotide state upon nutrient stimulation.

## Discussion

Nutrients signal to mTORC1 through the Rag GTPases, which receive inputs from the large, multiprotein GATOR1, KICSTOR, and GATOR2 complexes. Here, we determine that these factors stably assemble into the GATOR supercomplex, which is anchored to the lysosome by the Ragulator and Rag GTPases. These findings place the Rag GTPases at the center of both the physical architecture and signaling network of the mTORC1 nutrient-sensing pathway.

Several of our observations suggest that GATOR1, KICSTOR, and GATOR2 assemble into a single GATOR supercomplex. First, these three protein complexes share a requirement for Rag-Ragulator to access the lysosome; second, they are codependent on each other to associate with the lysosomal surface and remain associated to one another in the absence of lysosomal targeting; and third, their lysosomal abundances are coregulated by the nucleotide configuration of the Rag GTPases. The assembly of GATOR1, KICSTOR, and GATOR2 into the mammalian GATOR complex is reminiscent of the SEA complex in yeast, where SEACIT (GATOR1) and SEACAT (GATOR2) constitutively associate. Recent structural analysis of the SEA complex suggests that the SEACIT component tethers the holocomplex to the vacuole (38), in line with our observations that GATOR1 is required for GATOR2 and KICSTOR to access the lysosome.

While this manuscript was in preparation, Yan et al. reported that isoform 1 of ILF3 (ILF3i1), a predominantly nuclear protein, directly interacts with GATOR2 to recruit GATOR1 and GATOR2, but not KICSTOR, to the lysosome (39). Zhao et al., from the same research group, also suggested that lysosomal VWCE interacts with KICSTOR to selectively promote GATOR1, but not GATOR2 or KICSTOR, lysosomal recruitment (40). These results are both difficult to reconcile and surprising, given

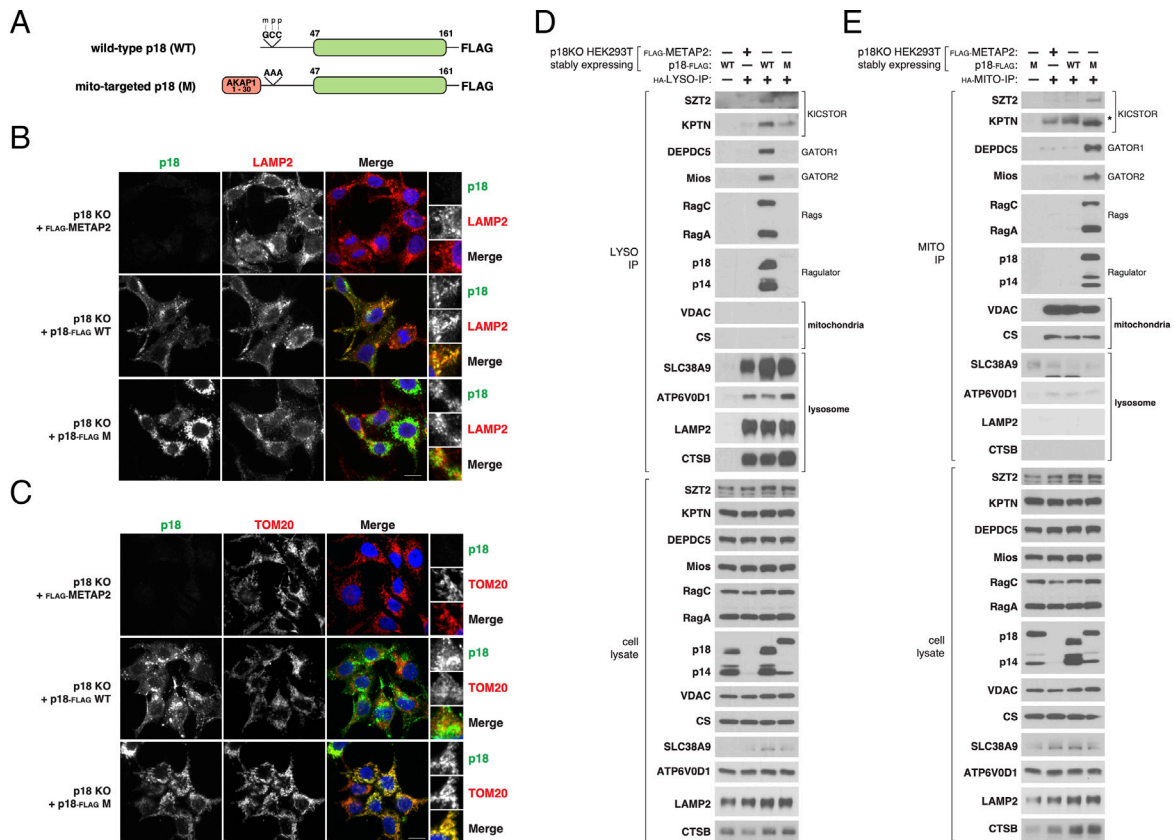


**Fig. 5.** Mito-targeted Ragulator recruits GATOR to the mitochondrial surface. (A) Schematic comparing wild-type (WT) and mito-targeted (M) p18. The mito-targeted p18 construct consists of AKAP1 residues 1 to 30 fused to a lipidation-deficient p18. m - myristoylation, p - palmitoylation. (B) Wild-type p18, but not mito-targeted p18, localizes to the lysosome. HEK293T cells of the indicated genotype were fixed and the Ragulator component p18 and LAMP2 were detected by immunofluorescence (The scale bar denotes 10 μm.) (C) Mito-targeted p18, but not wild-type p18, localizes to mitochondria. HEK293T cells of the indicated genotype were fixed and the Ragulator component p18 and TOM20 were detected by immunofluorescence (The scale bar denotes 10 μm.) (D) Expression of wild-type p18, but not mito-targeted p18, recruits the Rags and GATOR to the lysosome. Lysosomes were immunopurified from HEK293T cells of the indicated genotype expressing TMEM192-3xHA (HA-LYSO-IP) and analyzed by immunoblotting for the levels of the indicated proteins. (E) Expression of mito-targeted p18, but not wild-type p18, recruits the Rags and GATOR to mitochondria. Mitochondria were immunopurified from HEK293T cells of the indicated genotype and expressing 3xHA-EGFP-OMP25 (HA-MITO-IP) and analyzed by immunoblotting for the levels of the indicated proteins. Asterisk denotes non-specific bands.

that we report that GATOR2 requires KICSTOR to bind GATOR1 and GATOR1 to bind KICSTOR (Fig. 2 A–C) (15). In contrast, we find that GATOR1 and KICSTOR form a subcomplex that engages GATOR2 to associate with the lysosome in a Ragulator- and Rag-dependent manner. While ILF3 and VWCE are reported to be constitutively lysosomal, we show that relocalization of the Ragulator complex to the mitochondrial surface is sufficient to recruit GATOR to the mitochondria, implying that this function is independent of any potential role for lysosomal ILF3 or VWCE. Thus, although we cannot exclude the possibility that other factors help scaffold GATOR and its subcomplexes on the lysosome, our observations indicate that the evolutionarily conserved Rags and Ragulator are both necessary and sufficient for this function.

Unlike for GATOR, and in contrast to prior reports (41, 42), we find that the Rags and Ragulator are not required for the lysosomal localization of the TSC complex. Intriguingly, however, Demetriades et al. reported that the “inactive” form of the Rag GTPases most strongly immunoprecipitated TSC2. This observation may reflect an indirect interaction, consistent with the accumulation of Ragulator within detergent-resistant membranes (43) and our finding that the “inactive” Rag GTPases are most stably anchored to the lysosome.

Our results also indicate that GATOR consists of two intrinsically stable subcomplexes, GATOR1-KICSTOR and GATOR2, consistent with reports that KICSTOR is necessary for GATOR1

and GATOR2 to interact and that the S-adenosylmethionine sensor SAMTOR weakens the association between GATOR1-KICSTOR and GATOR2 (15, 22). It is presently unclear whether SAMTOR blocks formation of GATOR or simply weakens its integrity, so that it is more susceptible to disintegration during biochemical isolation.

We find that the nucleotide configuration of the Rag GTPases regulates the lysosomal accumulation of GATOR. Binding of GDP to Raga/B increases the lysosomal abundance of GATOR, likely by stabilizing both the Rag–Ragulator and Rag–GATOR interactions. Intriguingly, this suggests the existence of regulatory feedback between the GATOR complex and the Rags. Understanding the precise role of such feedback in nutrient control of mTORC1 signaling will likely depend on the specific molecular mechanism by which GATOR2 opposes GATOR1. Given the relative sizes of GATOR and the Rags, it is likely that a single GATOR complex interacts with several Rag GTPase heterodimers. Indeed, GATOR1 has been reported to interact with the Rag GTPases through at least two distinct binding modes, both of which may be important for GATOR to access the lysosome (12, 14), and we report here that Rag–Ragulator is substantially more abundant than GATOR.

Our results indicate that the Rag GTPases mediate the lysosomal recruitment of both their nutrient-gated regulator (GATOR) and effector (mTORC1). Similarly, the Rag–Ragulator heptamer recruits the FLCN–FNIP2 complex and the FLCN-dependent

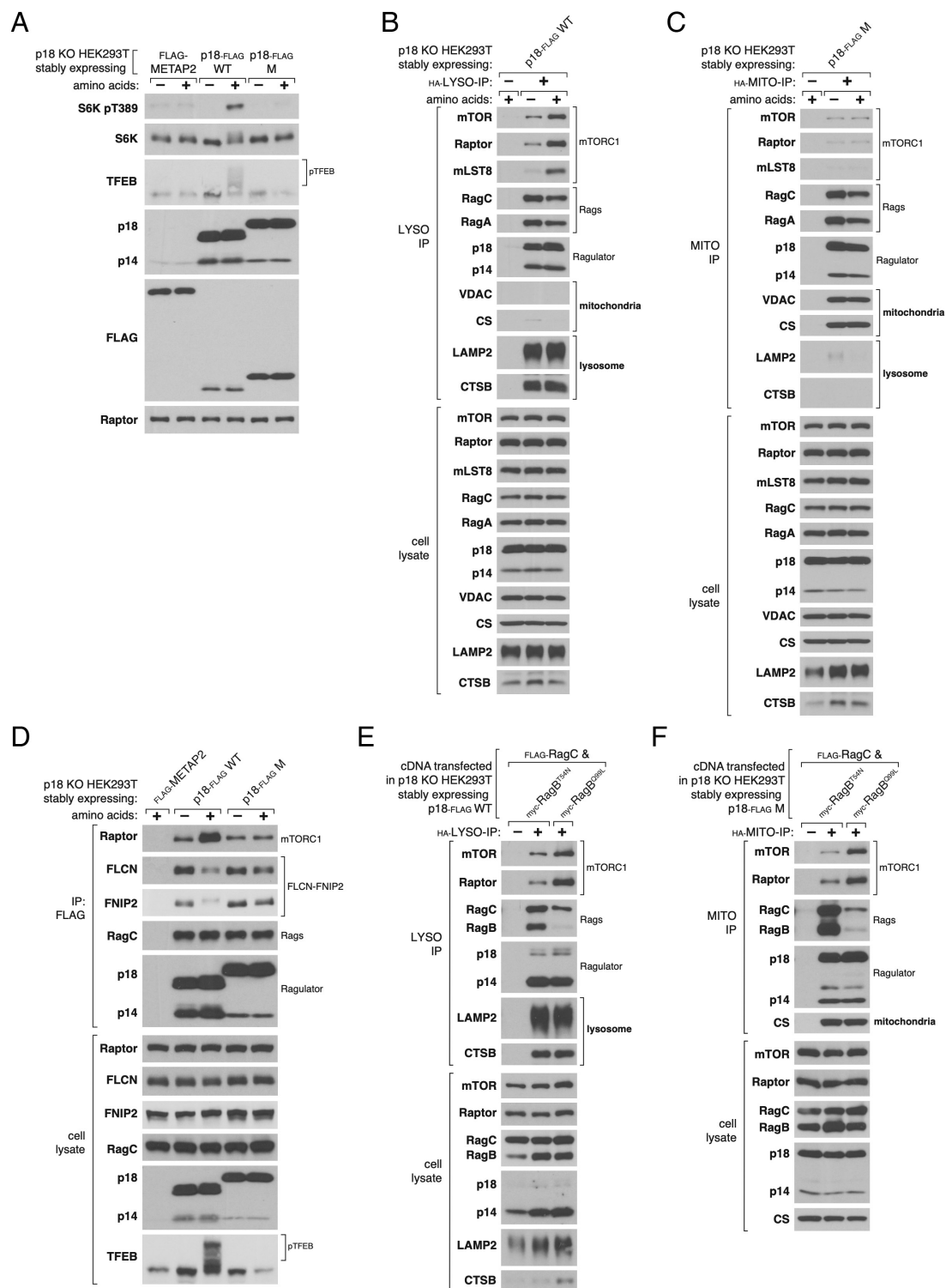


**Fig. 6.** Mitochondrial GATOR does not promote nutrient-dependent recruitment of mTORC1 to mitochondria. (A) Mito-targeted p18 does not promote amino acid-dependent phosphorylation of mTORC1 substrates. HEK293T cells of the indicated genotype were starved for amino acids for 60 min and restimulated or not with amino acids for 15 min prior to harvest. Cell lysates were analyzed by immunoblotting for the levels and phosphorylation states of the indicated proteins. (B) Amino acids stimulate recruitment of mTORC1 to the lysosome. p18-deficient HEK293T cells expressing wild-type p18 were starved for amino acids for 60 min and restimulated or not with amino acids for 15 min prior to harvest. Lysosomes were immunopurified from cells expressing TMEM192-3xHA (HA-LYSO-IP) and analyzed by immunoblotting for the levels of the indicated proteins. (C) In engineered cells, amino acids do not stimulate recruitment of mTORC1 to the mitochondria. p18-deficient HEK293T cells expressing mito-targeted p18 were starved for amino acids for 60 min and restimulated or not with amino acids for 15 min prior to harvest. Mitochondria were immunopurified from cells expressing 3xHA-EGFP-OMP25 (HA-MITO-IP) and analyzed by immunoblotting for the levels of the indicated proteins. (D) Amino acids do not promote the interaction between mito-targeted p18 and mTORC1. HEK293T cells of the indicated genotype were starved for amino acids for 60 min and restimulated with amino acids for 15 min prior to harvest. Anti-FLAG immunoprecipitates were prepared and analyzed by immunoblotting for the indicated proteins. (E) Expression of a GTP-loaded RagB mutant promotes recruitment of mTORC1 to the lysosome in cells expressing wild-type p18. Lysosomes were immunopurified from HEK293T cells expressing TMEM192-3xHA (HA-LYSO-IP) and analyzed by immunoblotting for the levels of the indicated proteins. (F) Expression of GTP-loaded RagB mutant promotes recruitment of mTORC1 to the mitochondria in cells expressing mito-targeted p18. Mitochondria were immunopurified from HEK293T cells expressing 3xHA-EGFP-OMP25 (HA-MITO-IP) and analyzed by immunoblotting for the levels of the indicated proteins.

mTORC1 substrates TFEB/TFE3 to the lysosome (25–27, 44–46). Thus, the role of the Rag GTPases extends beyond transducing nutrient cues to mTORC1. Each of these factors interacts with the Rag GTPases in a nutrient-regulated manner, which suggests the possibility of bidirectional communication between the Rag GTPases and their interaction partners. Similarly, nutrient availability governs the interactions between the Rag–Ragulator complex, SLC38A9, and the v-ATPase (32, 34–37, 47, 48). The Rag–Ragulator heptamer is necessary for gasdermin D-mediated pyroptosis and interacts with the lysosomal effluxer cystinosin (49–51). Unique among GTPases, the Rags are heterodimers that can occupy four distinct signaling states, only one of which predominantly interacts with mTORC1 (6–8, 52). It is therefore tempting to speculate that the Rag GTPase heterodimer functions as a general cellular nutrient sensor and that mTORC1 is only one of several Rag effectors.

The breadth and physical scale of the interacting partners of the Rag GTPases raises questions about the organization of the Rag-dependent signaling network on the lysosomal surface. For instance, what are the relative stoichiometries of the Rags and their host of interactors? Can a single Rag GTPase simultaneously accommodate multiple interactors? Are Rag GTPase heterodimers specialized, by posttranslational modification or otherwise, to exhibit distinct GTP hydrolysis kinetics (52) or to only engage certain partners? Recent work suggests that functional differences between RagA and RagB or RagC and RagD likely contribute to this signaling complexity (53, 54). It is likely that some Rag heterodimers are marked for dynamically regulated nucleotide exchange to convey information to mTORC1 (and other effectors) whereas other Rag heterodimers are static pillars that anchor regulators like GATOR to the lysosome.

Competition between regulators and effectors for binding to the Rag GTPases may also influence Rag-dependent signaling. Here, we show that overexpression of the SLC38A9 N-terminal domain displaces GATOR from the lysosome. These results reconcile the paradoxical observations that SLC38A9 functions as a GDI toward RagA/B *in vitro* but activates mTORC1 signaling when overexpressed (34–37). Indeed, we report that endogenous SLC38A9 is not required for mTORC1 to respond to the availability of all amino acids or, specifically, arginine. In contrast, disruption of the interaction between the cytosolic arginine sensor CASTOR1 and GATOR2 entirely eliminates the response of mTORC1 signaling to arginine availability (17, 21). Intriguingly, multiple groups have independently reported that transient loss of SLC38A9 blunts activation of mTORC1 by amino acids (34–36). Transient, but not stable, depletion of FLCN also impairs amino acid-induced S6K1 phosphorylation (24, 26). These results may reflect a temporary disequilibrium created upon acute loss of competitive Rag-interacting factors. While SLC38A9 has also been proposed to stimulate FLCN GAP activity (37), we find that SLC38A9-deficient cells, unlike those lacking FLCN, display no defects in TFEB phosphorylation. Combined with the recent finding that the Rag GTPase nucleotide state controls SLC38A9 amino acid transport (55), we speculate that SLC38A9 functions more as an effector, rather than a regulator, of the Rag GTPases. It is possible, however, that lysosomal efflux of leucine through SLC38A9 promotes mTORC1 activity through the cytosolic Sestrin1/2–GATOR2 axis.

Our findings establish that the lysosomal localization of mTORC1 is essential for it to sense amino acids. In contrast to a recent report (56), we find that complete loss of either RagA and B, RagC and D, or the Ragulator component p18 abolishes amino acid-dependent mTORC1 activation. Traditionally, generating clonal knockout cell lines requires single-cell dilution followed by

a period of clonal expansion and assessment for loss of expression. If insufficient time is allotted for expansion, slowly growing cell lines, such as those with complete loss of positive regulators of mTORC1, may not be represented in the array of recovered clones. Instead, those with incomplete knockdowns, functional truncations, or compensatory changes in the expression of other pathway components may predominate. To ensure recovery of complete, uncompensated knockouts, we screened candidate clones by genomic sequencing after a prolonged period of expansion and then verified loss of expression by long exposure immunoblotting. The results we obtained with these cell lines confirm that Ragulator and the Rag GTPases are essential for amino acids to activate mTORC1. In contrast, Fernandes et al. report that phosphorylation of lysosomal mTORC1 substrates (TFEB, TFE3) is more sensitive to the loss of the Rag GTPases than phosphorylation of cytosolic substrates (S6K1, 4EBP1) (56). These results may be explained by incomplete loss of the Rag GTPases, which would disproportionately affect the modification of lysosomal substrates that depend on Rag-mediated recruitment of both mTORC1 and the substrates themselves (57). Alternatively, compensatory upregulation of the Rheb GTPase expression or activity, which can promote S6K1 phosphorylation independently of lysosomal localization (58), could underlie these disparate observations, as has been previously observed in cells lacking the Rag GTPases (30). Last, we note that Fernandes et al. generated knockout lines in HEK293FT cells, a commercial clone selected for rapid proliferation and high protein expression, which may confound the study of growth control regulation.

Previous work has established that amino acids control the subcellular localization of mTORC1 in a Rag- and Ragulator-dependent manner (6, 9). Direct targeting of mTORC1 to a Rheb-containing compartment bypasses the need for Rag–Ragulator and is sufficient to stimulate phosphorylation of some, but not all, mTORC1 substrates. In contrast to that of S6K and 4EBP1, the phosphorylation of TFEB requires activated Rags and Ragulator but not Rheb (9, 25, 33, 57). These studies suggest that genetically engineered variants of mTORC1, which bypass nutrient signaling, are capable of catalyzing substrate phosphorylation on different organelles. Although limited evidence exists to support a role for native Rag–Ragulator function in other compartments, we explored here whether the nutrient-dependent GATOR–Rag pathway was able to function outside of its lysosomal context.

Although targeting of the Ragulator to the mitochondrial surface was sufficient to relocalize the Rags and GATOR, it did not recapitulate the nutrient-stimulated interaction between the Rag GTPases and mTORC1 or TFEB. Our results suggest that the mitochondrially localized Rag GTPases are not appropriately activated upon amino acid stimulation, which implies that their GATOR-dependent regulation is dysfunctional on the mitochondrial surface.

Several factors may contribute to this apparent dysregulation. For instance, the structural relationship between GATOR2 and membrane tethering complexes suggests that its activating function may be affected by membrane composition (17), which differs between the lysosomal and mitochondrial surfaces. Additionally, the Ragulator component p18 localizes to lipid rafts which may promote clustering of Rag–Ragulator heptamers in a way not recapitulated on the mitochondrial surface (43). The mitochondrial surface area is also much more extensive than that of lysosomes. These differences may particularly influence GATOR function if GATOR simultaneously engages multiple Rag–Ragulator heptamers, much like mTORC1 (7, 8) and TFEB (57). Indeed, depletion of GATOR1 from cells expressing mito-targeted p18 did not meaningfully increase recruitment of mTORC1 or

TFEB to the mitochondria, consistent with requirement for multiple adjacent Rag–Regulator complexes to stably dock each of these factors onto the membrane.

Retargeting of Regulator to the mitochondria also does not relocate either SLC38A9 or the v-ATPase, both of which are membrane proteins and interact with the Rag GTPases and Regulator. These, or other yet-to-be identified lysosome-specific factors, may be critical for proper regulation of the Rag nucleotide state. Finally, mTORC1 rapidly cycles between the cytosol and lysosome, suggesting the presence of dedicated trafficking pathways that are likely not optimized to promote mitochondrial localization (33). Collectively, these findings suggest that the mTORC1 nutrient-sensing pathway has evolved specifically to function on the lysosome, a recycling center and signaling hub within the cell.

## Materials and Methods

Reagents were obtained from the following sources: antibodies against S6K1 pT389 (9234), S6K1 (2708), MIO5 (13557), WDR59 (53385), NPRL2 (37344), RagA (4357), RagC (3360), RagD (4470), p18 (8975), p14 (8145), mTOR (2983), TSC2 (4308), CTSSB (31718), Sestrin2 (8487), VDAC (4866), Citrate Synthase (CS, 14309), TFEB (4240), mLST8 (3274), FLCN (3697), FNI2 (57612), Myc epitope tag (2278), Flag epitope tag (14793), HA epitope tag (3724), HRP-linked anti-mouse secondary antibody (7076), HRP-linked anti-rabbit secondary antibody (7074), and HRP-linked mouse anti-rabbit conformation specific secondary antibody (5127) were from Cell Signaling Technology; antibody against SZT2 was provided by Jianxin Xie of Cell Signaling Technology; antibodies against LAMP2 (sc-18822), CTSC (sc-74590), and TOM20 (sc-17764) were from Santa Cruz Biotechnology; antibodies against SEH1L (ab218531), ATP6V0d1 (ab202899), DEPDC5 (ab213181), and HRP-linked anti-mouse secondary antibody (ab131368) were from Abcam; antibody against SLC38A9 (NBP1-69235) was from Novus Biologicals; antibodies against WDR24 (20778-1-AP), KPTN (16094-1-AP), and Sestrin1 (21668-1-AP) were from Proteintech; antibody against SAMTOR (HPA050733) and Flag-M2 antibody (F1804) used for preparing anti-Flag magnetic beads were from Millipore Sigma; antibody against Raptor (09-217) was from EMD Millipore; Alexa 488, 568, and 647-conjugated secondary antibodies were from Invitrogen. Amino acids were from Millipore Sigma; DMEM, inactivated fetal serum (IFS), Dynabeads M-270 Epoxy, Dynabeads Protein G, and anti-HA magnetic beads were from Thermo Fisher Scientific; XtremeGene9 and Complete Protease Cocktail were from Roche; amino acid-free RPMI was from US Biologicals.

**Cell Lines and Tissue Culture.** Adherent HEK293T cells were cultured in DMEM (Thermo Fisher Scientific) with 10% IFS (Thermo Fisher Scientific) and 4.5 g/L glucose containing 2 mM GlutaMAX (Thermo Fisher Scientific), 100 IU/mL penicillin, and 100 µg/mL streptomycin. Adherent cell lines were maintained at 37 °C and 5% CO<sub>2</sub>. All cell lines were obtained from ATCC (American Type Culture Collection) and validated and tested for *Mycoplasma*.

**Transfections, Cell Lysis, and Immunoprecipitation Experiments.** Transfection, cell lysis, and immunoprecipitation were performed as previously described (15, 17). To harvest samples, cells were washed once with ice-cold PBS and then lysed with Triton X-100 lysis buffer (1% Triton X-100, 40 mM HEPES pH 7.4, 10 mM β-glycerol phosphate, 10 mM pyrophosphate, 2.5 mM MgCl<sub>2</sub>) and 1 tablet of EDTA-free protease inhibitor (Roche) per 25 mL buffer. Cell lysates were clarified by centrifugation at 21,000 × g at 4 °C for 10 min.

For anti-Flag immunoprecipitations, magnetic beads bound to the antibody recognizing the Flag epitope tag were prepared in-house by coupling Dynabeads M-270 Epoxy (Thermo Fisher Scientific) to Flag M2 antibody (Millipore Sigma) as previously described (59). Beads were washed three times with the Triton X-100 lysis buffer prior to use, and then incubated with the supernatant of each clarified lysate for 1 h at 4 °C. Each immunoprecipitation used 10 µL of anti-Flag Dynabeads. For endogenous immunoprecipitations, 4 µL of each primary antibody was added to each sample of clarified lysate and incubated at 4 °C for 1 h. Subsequently, 30 µL of prewashed Protein G Dynabeads was added to each sample and incubated for an additional 1 h at 4 °C. Following immunoprecipitation, beads were washed one time with Triton X-100 lysis buffer and two times with Triton X-100 lysis buffer supplemented to contain 150 to 500 mM NaCl. Immunoprecipitated proteins were denatured by addition of SDS-PAGE sample

buffer and boiling for 5 min at 95 °C. Immunoprecipitated proteins were then resolved by 4 to 20% SDS-PAGE before analysis by immunoblotting.

For experiments requiring transfection of cDNAs into HEK293T cells, 2 × 10<sup>6</sup> cells were plated in 10-cm culture dishes or 5 × 10<sup>6</sup> cells were plated in 15-cm culture dishes. 24 h later, cells were transfected with the appropriate pRK5-based cDNA expression plasmids using the polyethylenimine method, as previously described (60). The total amount of plasmid DNA in each transfection was normalized to 5 µg with empty pRK5 (10 cm plates) or 20 µg of empty pRK5 (15 cm plates). 36 h following transfection, cells were processed using the appropriate protocol.

For experiments which required amino acid starvation, cells were incubated in amino acid-free RPMI for 60 min, as previously described (11). To restimulate cells following starvation, an amino acid mixture prepared from individual powders of amino acids (Millipore Sigma) was added to cell culture media for 15 min. Starvations for individual amino acids were performed similarly.

**Immunopurification of Organelles.** Immunopurifications of lysosomes and mitochondria were performed from cells stably expressing either the HA-Lyso-IP tag (pLJC5-TMEM192-3xHA) or the HA-MITO-IP tag (pMXs-3xHA-EGFP-OMP25) (28, 29). Each sample was from three confluent 15 cm plates and was separately processed with regimented wash durations to maintain fast and reproducible immunopurification times. Briefly, cells were transitioned to nutrient-deficient or -replete media, as indicated in each figure, prior to harvest. Cells were washed once in ice-cold PBS and then scraped into 1 mL KPBS. Samples from multiple plates were pooled at this stage. Samples were pelleted by centrifugation at 1,000 × g at 4 °C for 2 min. Pelleted cells were resuspended in 950 µL KPBS supplemented with EDTA-free protease inhibitor (Roche) and 25 µL of the resuspended material was separated for analysis of whole cell lysate. Resuspended samples were homogenized with 25 strokes in a 2 mL dounce homogenizer. Homogenized material was centrifuged at 1,000 × g at 4 °C for 2 min and the supernatant was incubated with 100 µL of anti-HA magnetic beads for 3 min at 4 °C on a rotating shaker. Following capture, beads were washed three times with KPBS. Captured proteins were eluted by the addition of 50 µL Triton lysis buffer supplemented with EDTA-free protease inhibitor (Roche) followed by incubation for 10 min at 4 °C on a rotating shaker and centrifugation at 21,000 × g at 4 °C for 10 min. Eluted samples were separated from the beads and denatured by addition of SDS-PAGE sample buffer. To obtain whole cell lysate, the sample separated prior to homogenization was centrifuged at 1,000 × g at 4 °C for 2 min. Pelleted material was resuspended in 200 µL Triton lysis buffer supplemented with EDTA-free protease inhibitor (Roche), incubated for 10 min at 4 °C on a rotating shaker, and centrifugation at 21,000 × g at 4 °C for 10 min. The supernatant was denatured by addition of SDS-PAGE sample buffer. Samples were analyzed by immunoblotting, as described above. For experiments requiring transfection (Fig. 3B and 6E and F), cells were transfected two days prior to harvest, as described above.

**Immunofluorescence Assays.** Immunofluorescence imaging was performed as described previously (15, 22, 61). For the experiment in Fig. 1C, HEK293T cells with the indicated genetic backgrounds were counted, and then 400,000 cells from each cell line were evenly plated on fibronectin-coated glass coverslips (TED PELLA, Inc.) in 6-well plates. For the experiments in Fig. 5B and C, 400,000 HEK-293T cells of the indicated genotypes were plated on Poly-D-Lysine-coated glass coverslips in 6-well tissue culture plates. After 24 h, the coverslips were quickly rinsed once with PBS and fixed with 4% paraformaldehyde (PFA) in PBS at room temperature for 15 min. The coverslips were then rinsed three times with PBS to wash away remaining PFA and the cells were permeabilized with 0.05% Triton X-100 in PBS at room temperature for 5 min. After rinsing the coverslips three times with PBS, the cells were blocked for 1 h at room temperature in Odyssey blocking buffer (LI-COR). Then the coverslips were incubated with primary antibody cocktail in Odyssey blocking buffer at 4 °C overnight, rinsed three times with PBS, and incubated in the dark with corresponding secondary antibodies (diluted 1:500 in Odyssey blocking buffer) for 1 h at room temperature, and afterward washed three times with PBS. For samples in Figs. 5B and C, 8 µM of Hoechst 33342 (Thermo Fisher) was added to stain nuclei. The primary antibodies used were anti-WDR59 (CST; 1:250 dilution), anti-LAMP2 (Santa Cruz Biotechnology; 1:300 dilution), anti-p18 (CST; 1:500 dilution), anti-TOM20 (Santa Cruz Biotechnology; 1:1000 dilution). For Fig. 1C, coverslips were mounted on glass slides using Vectashield (Vector Laboratories) containing DAPI. For Fig. 5B and C, coverslips were mounted on glass slides using ProLong Gold Antifade mount (Invitrogen).

An Alexa488-conjugated secondary antibody was used for the WDR59 staining in Fig. 1C and the p18 staining in Fig. 5 B and C. The excitation wavelength was 488 nm. An Alexa568-conjugated secondary antibody was used for staining LAMP2 with an excitation wavelength of 561 nm.

A Zeiss AxioVert200M microscope was used to acquire images with a 63X or 100X oil immersion objective and a Yokogawa CSU-22 spinning disk confocal head with a Borealis modification (Spectral Applied Research/Andor) as well as a Hamamatsu ORCA-ER CCD camera, equipped at the Whitehead Institute Keck Imaging Center. The hardware and image acquisition were controlled by the MetaMorph software package (Molecular Devices). The excitation lasers used to capture the images were 405 nm, 488 nm, and 561 nm.

**cDNA Cloning.** To generate point mutants in cDNAs encoding NPRL2 or the Rag GTPases, site-directed mutagenesis reactions were performed using QuikChange kits (Agilent), according to the manufacturer's instructions.

The fusion construct expressing a version of p18 targeted to the mitochondria (p18-M) was synthesized as a gBlock gene fragment (Integrated DNA Technologies) containing the residues 1 to 30 of human AKAP1 joined by a flexible linker to residues 2 to 161 of human p18 containing the GCC to AAA substitution at residues 2 to 4, which disrupts the lipidation and lysosomal targeting (43, 62). Both this construct and a construct encoding wild-type p18 (p18-WT) were cloned into the pLJM1 vector with a C-terminal FLAG tag.

**Generation of Cells with Loss-of-Function Mutations in mTOR Pathway Components.** Generation of HEK293T cells lacking expression of mTOR pathway components was performed as previously described (15). The following oligonucleotide pairs were used to clone respective sgRNAs into the pX330 or pX458 vectors. Double knock-out cell lines were prepared sequentially.

```
sg_p18_S: caccgTGCTCATCAGTCCGAGCGGA
sg_p18_AS: aaacTCCGCTCGACATGATGAGCac
sg_RagA_S: caccgGTGGGAGTGTCCACGTCAA
sg_RagA_AS: aaacTTGACGTGGAACACTCCCAc
sg_RagB_S: caccgGAGCGGTTGTCTCGCCAT
sg_RagB_AS: aaacATGGGCGAGACAAACGCCTCc
sg_RagC_S: caccgAAAGGACTTCGGCTACGGCG
sg_RagC_AS: aaacCGCCGTAGCCGAAGTCTTTc
sg_RagD_S: caccgGCCGCTGTCCGATCGGCGT
sg_RagD_AS: aaacACGCCGATCCGACAGCGGCc
sg_SLC38A9_S: caccgTTTGTGGCTCTATACAGAA
sg_SLC38A9_AS: aaacTCTGTATAGAGCCACAAAc
sg_Mios_S: caccgTAGCAACGAAGATGCGTCTT
sg_Mios_AS: aaacAAGACGCATCTTCGTTGCTAc
sg_DEPDC5_S: caccgAAACCGAGCCTCAATTCGAC
sg_DEPDC5_AS: aaacGTCGAATTGAGGCTCGGTTTc
sg_SZT2_S: caccgCTCCGGCTCCGGCGCTCCG
sg_SZT2_AS: aaacCGGAGCGCCGGAGCCGGAGc
sg_Nprl2_S: caccgTGAAGAATATGCATTCGATG
sg_Nprl2_AS: aaacCATCGAATGCATATCTTCAc
```

For disruption of p18, RagA, RagB, RagC, RagD, SLC38A9, and Mios, guides were cloned into pX458. Following transfection, GFP-positive single cells were sorted into 96-well plates and allowed to expand for at least two weeks to ensure representation of slow-growing clones, as significant disruption of mTORC1 signaling was expected to impair cell fitness. All viable candidate clones were first validated in an unbiased manner by genomic sequencing. DNA from individual clones was extracted and specific, barcoded primers were used to amplify the genomic region targeted by each guide. Candidate knockout clones were selected following multiplexed amplicon sequencing and then validated by long exposure immunoblotting to confirm loss of the target protein(s).

The following primers were used to analyze genomic disruption:

```
sg_p18_seq_F: CTCTCCATGACCACTCTAGG
sg_p18_seq_R: GTCCTCTGACACTTACCTGGCT
sg_RagA_seq_F: GGCGGTGATGCCAAATACAG
sg_RagA_seq_R: CCATGAAGGTGTCCTGACC
sg_RagB_seq_F: GCTGATCAGTATGTGGGCTTT
sg_RagB_seq_R: TAAAATGAGGGAAGTCAAGGA
```

```
sg_RagC_seq_F: ACCATGTCCTGCAGTACG
sg_RagC_seq_R: CAGAATCCTCGGCTTGGGA
sg_RagD_seq_F: AGGAGGAGGAGGATGAGCTG
sg_RagD_seq_R: CTGGACCCCTCCAAGTC
sg_SLC38A9_seq_F: CTGACTTCCAGAAATTTTGGCT
sg_SLC38A9_seq_R: TGGTCACTAACCTCTGAATGA
sg_Mios_seq_F: ATCTTTAATGTGGGCTGTGGT
sg_Mios_seq_R: TGTGGATCTTCATTCCAGCTA
```

Disruption of DEPDC5 in cell lines expressing mito-targeted p18 (*SI Appendix, Fig. S4*) was performed using the Alt-R CRISPR-Cas9 system (Integrated DNA Technologies) following manufacturer protocol. Briefly, Cas9:sgRNA ribonucleoprotein (RNP) complexes were assembled in vitro and electroporated into HEK293T cells using a Lonza Nucleofactor X instrument, program CM-130. Cells were allowed to recover and validated by long exposure immunoblotting. The following crRNA sequence was used:

```
Hs.Cas9.DEPDC5.1.AA: TTAGTCGCCACATATCCCAA
```

**Generation of Cells Stably Expressing cDNAs.** Cells stably expressing cDNAs were generated as described previously (15, 28, 29). The following lentiviral expression plasmids were used: pLJM60-FLAG-METAP2, pLJC5-TMEM192-3xHA (Addgene #102930), pMXs-3xHA-EGFP-OMP25 (Addgene #83356), pLJM60-FLAG-NPRL2, pLJM60-FLAG-NPRL2 R78A, pLJM60-FLAG-SLC38A9.1 1-119 (Addgene #71862), pLJM1-p18-FLAG, pLJM1-AKAP1-p18AAA-FLAG, and pLJM1-FLAG-RagB Q99L (Addgene #19315).

**Generation of Cell Lines Endogenously Expressing 3xFLAG-Tagged mTORC1 Pathway Components.** Endogenously 3xFLAG-tagged cell lines were generated using Cas9:sgRNA ribonucleoprotein (RNP) complexes with asymmetric donor templates as previously described (63). Briefly, Cas9:sgRNA ribonucleoprotein (RNP) complexes were prepared in vitro and were electroporated into HEK293T cells, along with donor oligo, using a Lonza Nucleofactor X machine, protocol DN-100. Cells were allowed to recover and cloned. The following guides and donor oligos were used:

```
sg_p18: CCAAGGACCCCTCTCTCAT
```

```
p18-3C-3xFLAG:
```

```
CTTATGCTCA CAGTGC ACTTTCTCA GATCCGTGTGGA CGCAAAAGAGGA
GCTGGTGTGACA GTTTGG GATCCC ACTGGAAGTCT GTTCCAAGGACCAGA
CTA CAA AGA CCA TGA CGG TGATTATAA AGATCATGA CATCGATTA CAA GGA
TGACGATGACAAGTGAAGAGAGGGGCTCTTGACAGCTCTTCTCTCTC
```

```
sg_RagC: CGCCCCGACTGCAGGGACA
```

```
3xFLAG-3C-RagC:
```

```
A CTG GGG AGG CGG CGG CCT GGC TCG GCT TGG CCT GGC CTGTCA GGG
CGCGGG CGG CGG CTCCAG CACCATGGACTCAAAGACCATGACGGTGA
TTATAAAGATCATGACATCGATTACAAGGATGACGATGACAAAGCTGGAAGTTCT
GTCCAAGGACCATCCCTGCAGTACGGGGCGGAGGAGACGCCCTCGCC
```

```
sg_MIOS: ATCACATCAGTAACATGAG
```

```
3xFLAG-3C-MIOS:
```

```
CTTA GTT CTG AGT CAC ACA CAA CAA ATCTAT CAA CAT GGT GTG GTG CCC
ATA AAA TAT CAG GTTTGG TAC CGC TTG GTC CTT GGA ACA GAA CTT CCA GCT
TGT CAT CGT CAT CCT TGT AAT CGA TGT CAT GAT CTT TATA AT CAC CGT CAT
GGCTTTGTAGTCCATGTTACTGATGATGATCAAGGGTCCACTCAGGT
```

```
sg_DEPDC5: GTGCAAGATGAGACAACA
```

```
A AGA CCA ATC GAT ACT GAC CACTGC CCC CAA AGC CCT TCT TGT GGA
TGA CGA GTT TGT AGA CCT TTG TTG TTTG GTC CTT GGA ACA GAA CTT CCA
GCTTGT CAT CGT CAT CCTTGT AAT CGATGT CAT GAT CTTTATA AT CAC CGT CAT
GGCTTTGTAGTCCATCTGCAGTGTTCCTTTAGCTGTTCACAGC
```

```
3xFLAG-3C-DEPDC5:
```

The cell line expressing endogenously tagged 3xFLAG-SZT2 was generated as previously described (15).

sgRNAs cloned into pX330:

```
sg_SZT2_F: caccgGAGGGCTGTGTGATGGCCT
```

```
sg_SZT2_R: aaacAGGCCATCACAGCCCTCCc
```

single-stranded DNA oligo used for homologous recombination:

```
3xFLAG-SZT2: CAGGGGTCAAGAGTGGAAACCCCTCACTGCCCCGGCCGGCGC
GGGAGGCTGTGTGATGGACTACAAGACCATGACGGTGAATTATAAGATCATGACA
TTGATTACAAGGATGACGATGACAAGCGCGCCG CAGCGCCTCAGAGCGCCCGG
AGCCGGAGGTGAGGGCGGGCGGCGCAGCACTGGGCCCCGAGA.
```

**Data, Materials, and Software Availability.** All study data are included in the article and/or *SI Appendix*.

**ACKNOWLEDGMENTS.** We thank all members of the Sabatini Laboratory for helpful insights. This work was supported by grants to D.M.S. from the US NIH (R01 CA103866, R01 CA129105, and R01 AI47389), the Department of Defense (W81XWH-21-1-0260 and TS200035), the Lustgarten Foundation and the Leo Foundation, the Institute of Organic Chemistry and Biochemistry of the Czech Academy of Sciences, Pershing Square Philanthropies, and fellowship support from the NIH to M.L.V. and J.F.K. (T32 GM007753, F30 CA228229, F30 CA236179), and from the MIT School of Science Fellowship in Cancer Research to M.L.V. and from the Ludwig Center at MIT Graduate Student Fellowship and Damon Runyon Cancer Research Foundation (DRG-2469-22) to X.G. R.R.C. is supported by the Burroughs Wellcome Fund Career Award for Medical Scientists (CAMS) Award, the Ellison Foundation, the Smith Family Award for Excellence

1. A. J. Valvezan, B. D. Manning, Molecular logic of mTORC1 signalling as a metabolic rheostat. *Nat. Metabol.* **1**, 1–13 (2019).
2. C. H. Melick, J. L. Jewell, Regulation of mTORC1 by Upstream Stimuli. *Genes-Basel* **11**, 989 (2020).
3. J. Kim, K.-L. Guan, mTOR as a central hub of nutrient signalling and cell growth. *Nat. Cell Biol.* **21**, 63–71 (2019).
4. G. Y. Liu, D. M. Sabatini, mTOR at the nexus of nutrition, growth, ageing and disease. *Nat. Rev. Mol. Cell Biol.* **21**, 183–203 (2020).
5. A. González, M. N. Hall, Nutrient sensing and TOR signaling in yeast and mammals. *Embo J.* **36**, 397–408 (2017).
6. Y. Sancak *et al.*, The Rag GTPases bind raptor and mediate amino acid signaling to mTORC1. *Science* **320**, 1496–1501 (2008).
7. K. B. Rogala *et al.*, Structural basis for the docking of mTORC1 on the lysosomal surface. *Science* **366**, 468–475 (2019).
8. M. Anandapadamanaban *et al.*, Architecture of human Rag GTPase heterodimers and their complex with mTORC1. *Science* **366**, 203–210 (2019).
9. Y. Sancak *et al.*, Regulator-rag complex targets mTORC1 to the lysosomal surface and is necessary for its activation by amino acids. *Cell* **141**, 290–303 (2010).
10. S. Menon *et al.*, Spatial control of the TSC complex integrates insulin and nutrient regulation of mTORC1 at the lysosome. *Cell* **156**, 771–785 (2014).
11. L. Bar-Peled *et al.*, A tumor suppressor complex with GAP activity for the Rag GTPases that signal amino acid sufficiency to mTORC1. *Science* **340**, 1100–1106 (2013).
12. K. Shen *et al.*, Architecture of the human GATOR1 and GATOR1-Rag GTPases complexes. *Nature* **556**, 64–69 (2018).
13. K. Shen, M. L. Valenstein, X. Gu, D. M. Sabatini, Arg-78 of Npr12 catalyzes GATOR1-stimulated GTP hydrolysis by the Rag GTPases. *J. Biol. Chem.* **294**, jbc.AC119.007382–12 (2019).
14. S. B. Egri *et al.*, Cryo-EM structures of the human GATOR1-Rag-Regulator complex reveal a spatial-constraint regulated GAP mechanism. *Mol. Cell* **82**, 1836–1849.e5 (2022), 10.1016/j.molcel.2022.03.002.
15. R. L. Wolfson *et al.*, KICSTOR recruits GATOR1 to the lysosome and is necessary for nutrients to regulate mTORC1. *Nature* **543**, 438–442 (2017).
16. M. Peng, N. Yin, M. O. Li, SZT2 dictates GATOR control of mTORC1 signalling. *Nature* **543**, 433–437 (2017).
17. M. L. Valenstein *et al.*, Structure of the nutrient-sensing hub GATOR2. *Nature* **607**, 610–616 (2022).
18. R. L. Wolfson *et al.*, Sestrin2 is a leucine sensor for the mTORC1 pathway. *Science* **351**, 43–48 (2016).
19. R. A. Saxton *et al.*, Structural basis for leucine sensing by the Sestrin2-mTORC1 pathway. *Science* **351**, 53–58 (2015).
20. L. Chantranupong *et al.*, The CASTOR proteins are arginine sensors for the mTORC1 Pathway. *Cell* **165**, 153–164 (2016).
21. R. A. Saxton, L. Chantranupong, K. E. Knochenhauer, T. U. Schwartz, D. M. Sabatini, Mechanism of arginine sensing by CASTOR1 upstream of mTORC1. *Nature* **536**, 229–233 (2016).
22. X. Gu *et al.*, SAMTOR is an S-adenosylmethionine sensor for the mTORC1 pathway. *Science* **358**, 813–818 (2017).
23. H. R. Shin *et al.*, Lysosomal GPCR-like protein LYCHOS signals cholesterol sufficiency to mTORC1. *Science* **377**, 1290–1298 (2022).
24. Z.-Y. Tsun *et al.*, The folliculin tumor suppressor is a GAP for the RagC/D GTPases that signal amino acid levels to mTORC1. *Mol. Cell* **52**, 495–505 (2013).
25. G. Napolitano *et al.*, A substrate-specific mTORC1 pathway underlies Birt-Hogg-Dubé syndrome. *Nature* **585**, 597–602 (2020).
26. R. E. Lawrence *et al.*, Structural mechanism of a Rag GTPase activation checkpoint by the lysosomal folliculin complex. *Science* **366**, 971–977 (2019).
27. K. Shen *et al.*, Cryo-EM structure of the human FLCN-FNIP2-Rag-regulator complex. *Cell* **179**, 1319–1329.e8 (2019).
28. M. Abu-Remaih *et al.*, Lysosomal metabolomics reveals V-ATPase- and mTOR-dependent regulation of amino acid efflux from lysosomes. *Science* **358**, 807–813 (2017).
29. W. W. Chen, E. Freinkman, T. Wang, K. Birsoy, D. M. Sabatini, Absolute quantification of matrix metabolites reveals the dynamics of mitochondrial metabolism. *Cell* **166**, 1324–1337.e11 (2016).
30. A. Efeyan *et al.*, RagA, but Not RagB, is essential for embryonic development and adult mice. *Dev. Cell* **29**, 321–329 (2014).
31. Q. Huang, D. Szklarzyk, M. Wang, M. Simonovic, C. von Mering, PaxDb 5.0: Curated protein quantification data suggests adaptive proteome changes in yeasts. *Mol. Cell. Proteom.* **22**, 100640 (2023).
32. L. Bar-Peled, L. D. Schweitzer, R. Zoncu, D. M. Sabatini, Regulator 1s a GEF for the Rag GTPases that signal amino acid levels to mTORC1. *Cell* **150**, 1196–1208 (2012).
33. R. E. Lawrence *et al.*, A nutrient-induced affinity switch controls mTORC1 activation by its Rag GTPase-regulator lysosomal scaffold. *Nat. Cell Biol.* **20**, 1052–1063 (2018).
34. S. Wang *et al.*, Lysosomal amino acid transporter SLC38A9 signals arginine sufficiency to mTORC1. *Science* **347**, 188–194 (2015).
35. M. Rebsamen *et al.*, SLC38A9 is a component of the lysosomal amino acid sensing machinery that controls mTORC1. *Nature* **519**, 477–481 (2015).
36. J. Jung, H. M. Genau, C. Behrends, Amino Acid-Dependent mTORC1 Regulation by the Lysosomal Membrane Protein SLC38A9. *Mol. Cell Biol.* **35**, 2479–2494 (2015).
37. S. A. Fromm, R. E. Lawrence, J. H. Hurley, Structural mechanism for amino acid-dependent Rag GTPase nucleotide state switching by SLC38A9. *Nat. Struct. Mol. Biol.* **27**, 1017–1023 (2020).
38. L. Tafur *et al.*, Cryo-EM structure of the SEA complex. *Nature* **611**, 399–404 (2022).
39. G. Yan *et al.*, Genome-wide CRISPR screens identify IIF3 as a mediator of mTORC1-dependent amino acid sensing. *Nat. Cell Biol.* **25**, 754–764 (2023).
40. T. Zhao *et al.*, VWCV modulates amino acid-dependent mTOR signaling and coordinates with KICSTOR to recruit GATOR1 to the lysosomes. *Nat. Commun.* **14**, 8464 (2023).
41. C. Demetriades, N. Doumpas, A. A. Teleman, Regulation of TORC1 in response to amino acid starvation via lysosomal recruitment of TSC2. *Cell* **156**, 786–799 (2014).
42. S. Yang *et al.*, The Rag GTPase regulates the dynamic behavior of TSC downstream of both amino acid and growth factor restriction. *Dev. Cell* **55**, 272–288.e5 (2020).
43. S. Nada *et al.*, The novel lipid raft adaptor p18 controls endosome dynamics by anchoring the MEK-ERK pathway to late endosomes. *Embo J.* **28**, 477–489 (2009).
44. K. Li *et al.*, Folliculin promotes substrate-selective mTORC1 activity by activating RagC to recruit TFE3. *Plos Biol.* **20**, e3001594 (2022).
45. J. A. Martina, R. Puertollano, Rag GTPases mediate amino acid-dependent recruitment of TFE3 and MIF1 to lysosomes. *J. Cell Biol.* **200**, 475–491 (2013).
46. S. Wada *et al.*, The tumor suppressor FLCN mediates an alternate mTOR pathway to regulate browning of adipose tissue. *Gene Dev.* **30**, 2551–2564 (2016).
47. K. Shen, D. M. Sabatini, Regulator and SLC38A9 activate the Rag GTPases through noncanonical GEF mechanisms. *Proc. Natl. Acad. Sci. U.S.A.* **115**, 9545–9550 (2018).
48. R. Zoncu *et al.*, mTORC1 senses lysosomal amino acids through an inside-out mechanism that requires the vacuolar H<sup>+</sup>-ATPase. *Science* **334**, 678–683 (2011).
49. C. L. Evavold *et al.*, Control of gasdermin D oligomerization and pyroptosis by the regulator-rag-mTORC1 pathway. *Cell* **184**, 4495–4511.e19 (2021).
50. Z. Zheng *et al.*, The lysosomal Rag-Regulator complex licenses RIPK1- and caspase-8-mediated pyroptosis by Yersinia. *Science* **372**, eabg0269 (2021).
51. Z. Andrzejewska *et al.*, Cystinosin is a component of the vacuolar H<sup>+</sup>-ATPase-Ragulator-Rag complex controlling mammalian target of rapamycin complex 1 signaling. *J. Am. Soc. Nephrol.* **27**, 1678–1688 (2016).
52. K. Shen, A. Choe, D. M. Sabatini, Intersubunit cross talk in the Rag GTPase heterodimer enables mTORC1 to respond rapidly to amino acid availability. *Mol. Cell* **68**, 552–564.e9 (2017).
53. P. Gollwitzer, N. Grützmaker, S. Wilhelm, D. Kümmel, C. Demetriades, A Rag GTPase dimer code defines the regulation of mTORC1 by amino acids. *Nat. Cell Biol.* **24**, 1394–1406 (2022).
54. G. Figlia *et al.*, Brain-enriched RagB isoforms regulate the dynamics of mTORC1 activity through GATOR1 inhibition. *Nat. Cell Biol.* **24**, 1407–1421 (2022).
55. J. F. Kedir, “Regulation of amino acid transport across the lysosomal surface by the mTORC1 pathway,” (Massachusetts Institute of Technology, Cambridge, MA, 2022). Accessed 13 March 2023.
56. S. A. Fernandes *et al.*, Spatially and functionally distinct mTORC1 entities orchestrate the cellular response to amino acid availability. *BioRxiv [Preprint]* (2023), 10.1101/2023.10.03.559930 (Accessed 1 November 2023).
57. Z. Cui *et al.*, Structure of the lysosomal mTORC1-TFE3-Rag-Regulator megacomplex. *Nature* **614**, 572–579 (2023).
58. B. Angarola, S. M. Ferguson, Weak membrane interactions allow Rheb to activate mTORC1 signaling without major lysosome enrichment. *Mol. Biol. Cell* **30**, 2750–2760 (2019).
59. I. M. Cristea, B. T. Chait, Conjugation of magnetic beads for immunoprecipitation of protein complexes. *Cold Spring Harb. Protoc.* **2011**, pdb.prot5610 (2011).
60. O. Boussif *et al.*, A versatile vector for gene and oligonucleotide transfer into cells in culture and in vivo: Polyethylenimine. *Proc. Natl. Acad. Sci. U.S.A.* **92**, 7297–7301 (1995).
61. X. Gu *et al.*, Sestrin mediates detection of and adaptation to low-leucine diets in *Drosophila*. *Nature* **608**, 209–216 (2022).
62. Y. Jun *et al.*, D-AKAP1a is a signal-anchored protein in the mitochondrial outer membrane. *FEBS Lett.* **590**, 954–961 (2016).
63. C. D. Richardson, G. J. Ray, M. A. DeWitt, G. L. Curie, J. E. Corn, Enhancing homology-directed genome editing by catalytically active and inactive CRISPR-Cas9 using asymmetric donor DNA. *Nat. Biotechnol.* **34**, 339–344 (2016).

in Biomedical Research, and the MGH Department of Medicine Transformative Scholar Award.

Author affiliations: <sup>3</sup>Department of Medicine, Massachusetts General Hospital, Boston, MA 02114; <sup>4</sup>Whitehead Institute for Biomedical Research, Cambridge, MA 02142; <sup>5</sup>Department of Biology, Massachusetts Institute of Technology, Cambridge, MA 02139; <sup>6</sup>Harvard Medical School, Boston, MA 02115; <sup>7</sup>Department of Pathology, Massachusetts General Hospital, Boston, MA 02114; <sup>8</sup>Department of Pathology and Laboratory Medicine, Brown University, Providence, RI 02903; <sup>9</sup>Brown Center on the Biology of Aging, Brown University, Providence, RI 02903; <sup>10</sup>Legorreta Cancer Center, Brown University, Providence, RI 02903; <sup>11</sup>Center for Genomic Medicine, Massachusetts General Hospital, Boston, MA 02114; <sup>12</sup>Department of Surgery, Massachusetts General Hospital, Boston, MA 02114; <sup>13</sup>Broad Institute of Harvard and the Massachusetts Institute of Technology, Cambridge, MA 02142; and <sup>14</sup>Institute of Organic Chemistry and Biochemistry of the Czech Academy of Sciences, Prague 166 10, Czech Republic

Author contributions: M.L.V., P.V.L., X.G., and D.M.S. designed research; M.L.V., P.V.L., X.G., and J.F.K. performed research; J.F.K. and M.S.T. contributed new reagents/analytic tools; M.L.V., P.V.L., X.G., R.R.C., and D.M.S. analyzed data; and M.L.V. and D.M.S. wrote the paper.